Non-convex blind deconvolution approach for sparse radio-interferometric imaging

Audrey Repetti, Jasleen Birdi, and Yves Wiaux
Institute of Sensors, Signals and Systems, Heriot-Watt University, Edinburgh EH14 4AS, UK.

***Abstract*—New generations of imaging devices aim to produce high resolution and high dynamic range images. In this context, the associated high dimensional inverse problems can become extremely challenging from an algorithmic view point. In addition, the imaging procedure can be affected by unknown calibration kernels. This leads to the need of performing joint image reconstruction and calibration, and thus of solving non-convex blind deconvolution problems. In the recently submitted paper [1], we developed a method to solve the joint imaging and calibration problem in radio interferometry in astronomy. To solve this problem, we leverage a block-coordinate forward-backward algorithm, specifically designed to minimize non-smooth non-convex and high dimensional objective functions. Here we describe the proposed method and show its performance through simulation results.**

I. Introduction

In image processing, the objective is to find an estimation of an original unknown image $\overline{\boldsymbol{x}} \in \mathbb{R}^N$ from an inverse problem $\boldsymbol{y} = \overline{\boldsymbol{G}}\overline{\boldsymbol{x}} + \boldsymbol{w}$, where $\overline{\boldsymbol{G}}$ is an observation matrix and $\boldsymbol{w}$ is a realisation of an additive random noise. When $\overline{\boldsymbol{G}}$ is perfectly known, this problem can be efficiently solved using convex optimization tools [2], [3]. However, in practice, $\overline{\boldsymbol{G}}$ is unknown and has to be calibrated, jointly with the estimation of the image, leading to a blind deconvolution problem. The latter is a challenging task, mainly due to the non-linearity of the measurements, and, in the context of astronomical radio-interferometry, this difficulty is multiplied manifold by the high dimensionality of the underlying problem. Indeed, in this case, the images of interest can reach gigapixel or terapixel size, while the calibration variables correspond to a large number of low resolution images related to each antenna of the telescope [4], [5]. In this context adapted scalable approaches have to be developed.

II. Proposed blind deconvolution approach

In radio-interferometry, the observations consists of under-sampled Fourier measurements, acquired by antenna pairs indexed by $(\alpha, \beta) \in \{1, \ldots, n_a\}^2$, with $\alpha \neq \beta$ and n_a being the number of antennas of the interferometer. These acquisitions are degraded by antenna-based gains, acting as convolution kernels in the Fourier domain, and which can be modelled as low resolution complex valued images of dimension N. In this context, the objective is to estimate jointly the original unknown image $\overline{\boldsymbol{x}}$ and the direction dependent (DD) gain associated with each antenna. In order to reduce the dimensionality of this problem, we assume that for each antenna α, the associated gain is band-limited and consists in only $S \ll N$ non-zero coefficients in the Fourier domain, stored in a vector $\overline{\boldsymbol{u}}_\alpha \in \mathbb{C}^S$. Under this assumption, the measurements can be written as a data matrix $\boldsymbol{Y} = \overline{\boldsymbol{D}}_1 \overline{\boldsymbol{X}} \overline{\boldsymbol{D}}_2^\top + \boldsymbol{W}$, where $\overline{\boldsymbol{X}} \in \mathbb{C}^{N \times N}$ is the symmetric matrix containing on each line/row a translation of the Fourier transform of $\overline{\boldsymbol{x}}$, to model a convolution operation, $\boldsymbol{W}$ is a realization of an additive i.i.d. Gaussian noise matrix, and $\overline{\boldsymbol{D}}_1 \in \mathbb{C}^{n_a \times N}$ (resp. $\overline{\boldsymbol{D}}_2 \in \mathbb{C}^{n_a \times N}$) is the sparse matrix containing on each line the non-zero coefficients $\overline{\boldsymbol{u}}_{\alpha,1} = (\overline{u}_\alpha(-s))_s \in \mathbb{C}^S$ (resp. $\overline{\boldsymbol{u}}_{\alpha,2} = \overline{\boldsymbol{u}}_\alpha^*$), centred at the measured frequencies. Furthermore, we make use of prior information on bright sources of the image by considering $\overline{\boldsymbol{x}}$ as a sum of two images $\boldsymbol{b} + \overline{\boldsymbol{\epsilon}}$, where $\boldsymbol{b}$, with support $\mathcal{S}$, is known, while $\overline{\boldsymbol{\epsilon}}$ has to be estimated. Then, we propose to estimate jointly $\overline{\boldsymbol{\epsilon}}$, and matrices $\overline{\boldsymbol{D}}_1$ and $\overline{\boldsymbol{D}}_2$ defining their estimates as a solution to

$$\underset{\boldsymbol{\epsilon}, (\boldsymbol{u}_{\alpha,1}, \boldsymbol{u}_{\alpha,2})_{1 \leqslant \alpha \leqslant n_a}}{\text{minimize}} \quad F\left(\boldsymbol{\epsilon}, (\boldsymbol{u}_{\alpha,1}, \boldsymbol{u}_{\alpha,2})_{1 \leqslant \alpha \leqslant n_a}\right) + R(\boldsymbol{\epsilon}) + \sum_{\alpha=1}^{n_a} P_\alpha(\boldsymbol{u}_{\alpha,1}, \boldsymbol{u}_{\alpha,2}), \tag{1}$$

where F is the data fidelity term chosen to be a least squares criterion related to the observation model, and R (resp. P_α) is the regularization term to incorporate *a priori* information in the image (resp. DD gains). On the one hand, we use R to promote sparsity (using an ℓ_1 norm) in the restriction of $\boldsymbol{\epsilon}$ to the complementary set $\mathcal{S}^c$ of $\mathcal{S}$, leveraging recent results in the compressive sensing theory [6]. Moreover, we consider a positivity constraint in $\mathcal{S}^c$, while, in $\mathcal{S}$, we use bounds related to the possible errors appearing in $\boldsymbol{b}$. On the other hand, $\overline{\boldsymbol{D}}_1$ and $\overline{\boldsymbol{D}}_2$ corresponding to the same coefficients up to a transformation, we choose P_α to control the distance between $\boldsymbol{u}_{\alpha,1}$ and $\boldsymbol{u}_{\alpha,2}$. Moreover, we consider constraints on the amplitude of the Fourier coefficients of the DD gains.

We propose to solve the non-convex non-smooth minimization problem (1) using an alternating forward-backward approach based on the algorithm proposed in [7], which comes with convergence guarantees. Basically, this iterative algorithm alternates between the estimation of the image $\boldsymbol{\epsilon}$ and the estimation of variables $(\boldsymbol{u}_{\alpha,1}, \boldsymbol{u}_{\alpha,2})_{1 \leqslant \alpha \leqslant n_a}$ related to the DD gains, computing a gradient step followed by a proximity step. More details on the model and the method are given in [1].

III. Simulation results

To show the performance of the proposed approach, we computed numerical experiments on simulated sky images of size 128×128, consisting of point sources, generated randomly on two intensity levels, considering $n_a = 200$ randomly distributed antennas, and modelling DD gains with support of size $S = 7 \times 7$. More precisely $\overline{\boldsymbol{x}} = \overline{\boldsymbol{x}}_1 + \overline{\boldsymbol{x}}_2$, where $\overline{\boldsymbol{x}}_1$ is approximately known and has an energy $\mathsf{E}(\overline{\boldsymbol{x}}_1) = 10$, while $\overline{\boldsymbol{x}}_2$ is unknown and has a lower energy $\mathsf{E}(\overline{\boldsymbol{x}}_2)$, which we take to be either equal to 0.01, 0.1 or 1. The approximation $\boldsymbol{b}$ of $\overline{\boldsymbol{x}}_1$ is modelled such that $b(n) = (1 + pz(n))x_1(n)$ where $z(n) \sim \mathcal{N}(0, 1)$, and $p > 0$ determines the approximation degree of $\overline{\boldsymbol{x}}_1$. Then, the objective is to estimate the faint sources belonging to $\overline{\boldsymbol{x}}_2$. In Fig. 1 is shown the true second level $\overline{\boldsymbol{x}}_2$ (left), its estimations considering $p = 0.01$ (center), and $p = 0.1$ (right). We can observe that in the cases when $\mathsf{E}(\overline{\boldsymbol{x}}_2) \in \{0.1, 1\}$, the positions of the faint sources are recovered correctly. When $\mathsf{E}(\overline{\boldsymbol{x}}_2) = 0.01$, the reconstruction is less accurate. However, it is worth noting that in this case the errors considered between $\boldsymbol{b}$ and $\overline{\boldsymbol{x}}_1$ are 10 to 100 times larger than the intensity of sources in $\overline{\boldsymbol{x}}_2$. Moreover, we compare our approach with a state of the art method [8] for direction independent effects calibration in radio-interferometry, where DD gains are approximated by constant images instead of low-resolution images. However, contrary to our method, [8] does not provide any sensible reconstruction of $\overline{\boldsymbol{x}}_2$. These results are attested by Fig. 2 which shows an SNR comparison of the reconstruction of $\overline{\boldsymbol{x}}_2$ using both methods.

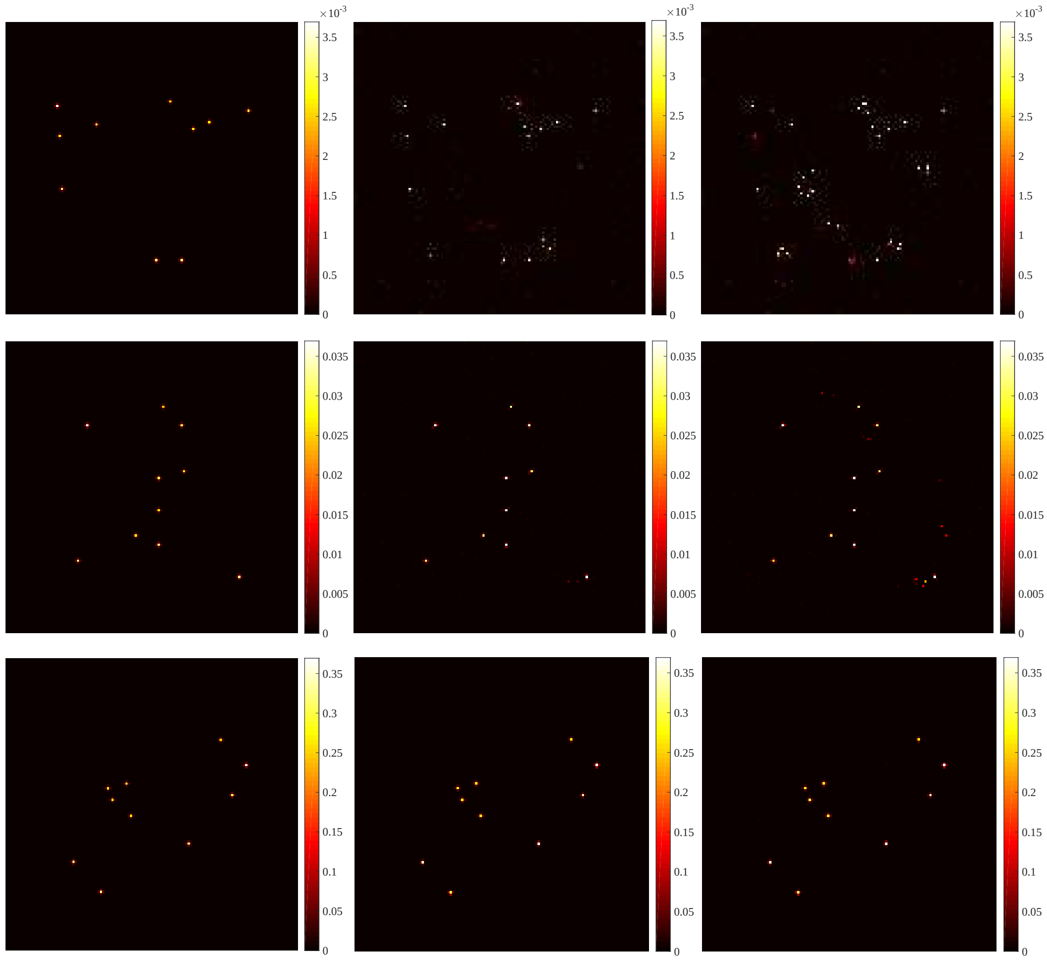

Figure 1. Top row: (left) True $\overline{\boldsymbol{x}}_2$ with energy $\mathsf{E}(\overline{\boldsymbol{x}}_2) = 0.01$, and reconstructions obtained using the proposed method considering (center) $p = 0.01$ and (right) $p = 0.1$. Middle row: (left) True $\overline{\boldsymbol{x}}_2$ with energy $\mathsf{E}(\overline{\boldsymbol{x}}_2) = 0.1$, and reconstructions obtained using the proposed method considering (center) $p = 0.01$ and (right) $p = 0.1$. Bottom row: (left) True $\overline{\boldsymbol{x}}_2$ with energy $\mathsf{E}(\overline{\boldsymbol{x}}_2) = 1$, and reconstructions obtained using the proposed method considering (center) $p = 0.01$ and (right) $p = 0.1$.

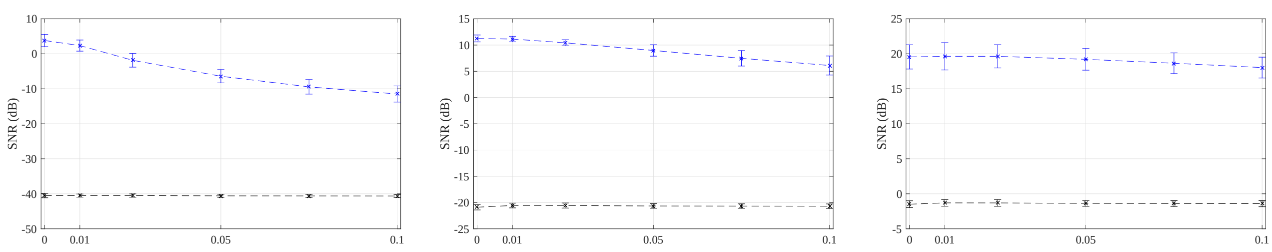

Figure 2. SNR values of the reconstructed second level $\overline{\boldsymbol{x}}_2$ obtained varying $p \in \{0, 0.01, 0.025, 0.05, 0.075, 0.1\}$ and considering (left) $\mathsf{E}(\overline{\boldsymbol{x}}_2) = 0.01$, (center) $\mathsf{E}(\overline{\boldsymbol{x}}_2) = 0.1$ and (right) $\mathsf{E}(\overline{\boldsymbol{x}}_2) = 1$. Black curves are obtained using method [8], and blue curves corresponds to the reconstructions obtained using the proposed method. Results are given for an average over 10 realisations varying the antenna distribution, the random image, the approximation $\boldsymbol{b}$, and the DD gains.

References

[1] A. Repetti, J. Birdi, A. Dabbech, and Y. Wiaux, "A non-convex optimization algorithm for joint DDE calibration and imaging in radio interferometry," Tech. Rep., Jan. 2017, https://arxiv.org/abs/1701.03689.

[2] P. L. Combettes and J.-C. Pesquet, "Proximal splitting methods in signal processing," in *Fixed-Point Algorithms for Inverse Problems in Science and Engineering*, H. H. Bauschke, R. Burachik, P. L. Combettes, V. Elser, D. R. Luke, and H. Wolkowicz, Eds. New York: Springer-Verlag, 2010, pp. 185–212.

[3] Y. Wiaux, L. Jacques, A. M. M. Puy, G.and Scaife, and P. Vandergheynst, "Compressed sensing imaging techniques for radio interferometry," *Mon. Not. R. Astron. Soc.*, vol. 395, pp. 1733–1742, 2009.

[4] O. Smirnov, "Revisiting the radio interferometer measurement equation. ii. calibration and direction-dependent effects," *A & A*, vol. 527, no. A107, p. 10, March 2015.

[5] A. Onose, R. E. Carrillo, A. Repetti, J. D. McEwen, J.-P. Thiran, J.-C. Pesquet, and W. Y., "Scalable splitting algorithms for big-data interferometric imaging in the ska era," *Mon. Not. R. Astron. Soc.*, vol. 462, pp. 4314–4335, 2016.

[6] L. Jacques, "A short note on compressed sensing with partially known signal support," *Sign. Process.*, vol. 90, pp. 3308–3312, 2010.

[7] E. Chouzenoux, J.-C. Pesquet, and A. Repetti, "A block coordinate variable metric forward-backward algorithm," *J. Global Optim.*, vol. 66, no. 3, pp. 457–485, Nov. 2016.

[8] S. Salvini and S. J. Wijnholds, "Fast gain calibration in radio astronomy using alternating direction implicit methods: Analysis and applications," *A&A*, vol. 571, p. A97, 2014.